Geophysical Prospecting 34, 1067–1081, 1986.

GEOELECTRIC DETERMINATION OF QUALITY CHANGES AND TECTONIC DISTURBANCES IN COAL DEPOSITS*

J. CSÓKÁS, M. DOBRÓKA and Á. GYULAI**

ABSTRACT

CSÓKÁS, J., DOBRÓKA, M. and GYULAI, Á. 1986, Geoelectric Determination of Quality Changes and Tectonic Disturbances in Coal Deposits, Geophysical Prospecting 34, 1067–1081.

A new underground geoelectric method is presented for the determination of small tectonic disturbances and barrenings in coal seams. The distribution of the apparent resistivity can be mapped from the measured apparent resistance data by using a recently developed geoelectric imaging method. The applicability of the methods are proved by in situ measurements and by a model experiment.

INTRODUCTION

Efficiency and safety of coal mining necessitate that the tectonic and stratigraphic features of the coal deposits should be well known. By surface geophysics this information is generally not obtainable with sufficient accuracy. If one hits a fault, a pinch-out, or a dirt bed during coal-drawing, this would probably not only reduce the output, but could even cause a water inrush. Tectonic disturbances of coal series are traced by openings and headings, but these methods are expensive. However, there are geophysical methods for which the necessary measurements are carried out within the mine, and by which even smaller disturbances of the coal series can be detected (in-seam seismic reflection and transmission methods were described by Mason, Buchanan and Bover 1980, Dresen and Freystätter 1976, Krey, Arnetzl and Knecht 1982).

IN-SEAM GEOELECTRIC METHODS

Two new methods called 'geoelectric seam-sounding and transillumination' allow the determination of tectonic and stratigraphic disturbances of coal beds. Both are

* Paper presented at the 47th meeting of the EAEG, Budapest, June 1985, revision accepted May 1986.

** Technical University of Heavy Industries, Department of Geophysics, 3515 Miskolc-Egyetemváros, Hungary.

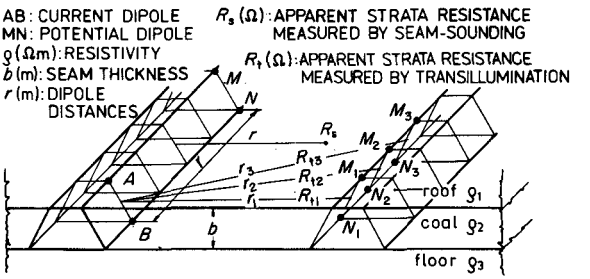

Fig. 1. The dipole array for seam-sounding and transillumination.

based on the fact that a coal bed is a layer of high resistivity embedded in a medium of considerably lower resistivity. In the fault zones the roof and floor layers (of much lower resistivity) get connected, so that the apparent resistance of the medium measured by an equatorial dipole array is lower than it would be in its undisturbed position (Csókás 1974). This decrease in apparent resistance allows one to detect the tectonic disturbances.

The principle of the methods is shown in fig. 1. The current electrodes A and B and the potential electrodes M and N are placed at the upper and lower boundaries of the coal seam in an equatorial dipole array. For *seam-sounding* the dipoles are placed in the same drift. The distance r between the dipoles is gradually expanded during sounding. If two drifts are accessible in the investigated area, we can use geoelectric seam-transillumination. In this case the current dipole is placed in one of the drifts and the potential dipole in the other. The dipole array should cover the bed in a fan-shaped form as far as possible. The apparent resistance R_s of an undisturbed coal series can be calculated from the potential functions (van Nostrand 1966) using the principle of additivity of the potentials.

The three-layer case is described by the following equation (Csókás 1974):

$$R_s = \frac{U}{I} = \frac{\rho_1 + \rho_3}{4\pi r}\left\{1 + \frac{\rho_1 k_{21} + \rho_3 k_{23}}{\rho_1 + \rho_3}\sum_{n=0}^{\infty}\frac{(k_{21}k_{23})^n \frac{r}{b}}{\left[4n^2 + \left(\frac{r}{b}\right)^2\right]^{1/2}}\right.$$

$$- \frac{\rho_1 k_{23} + \rho_3 k_{21}}{\rho_1 + \rho_3}\sum_{n=0}^{\infty}\frac{(k_{21}k_{23})^n \frac{r}{b}}{\left[4(n+1)^2 + \left(\frac{r}{b}\right)^2\right]^{1/2}}$$

$$\left. - [1 - k_{21}k_{23} + k_{13}(k_{21} - k_{23})]\sum_{n=0}^{\infty}\frac{(k_{21}k_{23})^n \frac{r}{b}}{\left[4(n+0.5)^2 + \left(\frac{r}{b}\right)^2\right]^{1/2}}\right\}, \qquad (1)$$

where ρ_1, ρ_2 and ρ_3 are resistivities of the roof, coal bed and the floor, respectively, r is the distance between the dipoles, and b is the thickness of the bed. The resistivity

contrasts are denoted by

$$k_{ij} = \frac{\rho_i - \rho_j}{\rho_i + \rho_j},$$

where $i, j = 1, 2, 3$.

The results of seam-sounding are conveniently represented in log–log scale with R_s being plotted against r as shown in fig. 2.

By means of fitting the measured and computed curves with expression (1) we can decide whether the coal bed is tectonically undisturbed. In case of a proper fit between computed and measured curves the seam is undisturbed. Otherwise, a tectonically or stratigraphically disturbed zone is present. Experiences has shown that the distance between the fault zone and the surveyed part of the drift is equal to the dipole distance r for which the measured apparent resistance is 10% less than the computed one (fig. 2). In order to evaluate the data it is useful to prepare an album of master curves, as seen in fig. 3.

The equations of apparent resistance of undisturbed coal series can also be derived in case of multi-layered models. For example, when the floor consists of two layers, the first of thickness b' and resistivity ρ_3, the second having an infinite thickness and a resistivity ρ_4, the apparent resistance of the coal series is

$$\begin{aligned} R_s = \frac{U}{I} = \frac{\rho_2}{4\pi r} \cdot \frac{r}{b} \cdot \frac{1 - k_{21}}{k_{21}} \\ \times \left\{ \frac{b}{r} - \frac{1}{\left[\left(\frac{r}{b}\right)^2 + 1\right]^{1/2}} - \frac{k_{21}^2}{1 - k_{21}} \sum_{n=0}^{\infty} \frac{c_n}{\left[\left(\frac{2n}{P_1} + 2\right)^2 + \left(\frac{r}{b}\right)^2\right]^{1/2}} \right. \\ - k_{21} \sum_{n=0}^{\infty} \frac{c_n}{\left[\left(\frac{2n}{P_1} + 1\right)^2 + \left(\frac{r}{b}\right)^2\right]^{1/2}} - \frac{k_{21}}{1 - k_{21}} \sum_{n=0}^{\infty} \frac{b_n}{\left[\left(\frac{2n}{P_1}\right)^2 + \left(\frac{r}{h}\right)^2\right]^{1/2}} \\ + \frac{1}{1 - k_{21}} \sum_{n=0}^{\infty} \frac{b_n}{\left[\left(\frac{2n}{P_1} - 1\right)^2 + \left(\frac{r}{b}\right)^2\right]^{1/2}} + \frac{k_{21}}{1 - k_{21}} \sum_{n=0}^{\infty} \frac{c_n}{\left[\left(\frac{2n}{P_1}\right)^2 + \left(\frac{r}{b}\right)^2\right]^{1/2}} \\ \left. - \sum_{n=0}^{\infty} \frac{b_n}{\left[\left(\frac{2n}{P_1}\right)^2 + \left(\frac{r}{b}\right)^2\right]^{1/2}} \right\}, \end{aligned} \tag{2}$$

where the thickness of the series $b = P_1 H_0$ and $b' = P_4 H_0$, and b_n and c_n can be calculated by means of the recursive formulae

$$\begin{aligned} b_n + b_{n-P_4} k_{23} k_{34} - b_{n-P_1} k_{21} k_{23} \\ - b_{n-P_1-P_4} k_{21} k_{34} &= 1 - k_{21}, && \text{if } n = 0, \\ &= k_{23} k_{34} (1 - k_{21}), && \text{if } n = P_4, \\ &= 0, && \text{if } n \neq 0 \neq P_4 \end{aligned}$$

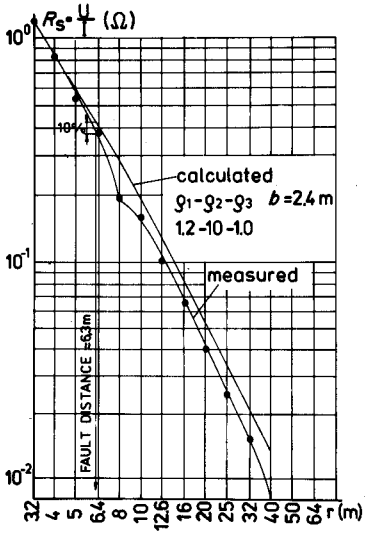

Fig. 2. Comparison of measured and calculated seam-sounding curves.

$$c_n + c_{n-P_4}k_{23}k_{34} - c_{n-P_1}k_{21}k_{23} - c_{n-P_4-P_1}k_{21}k_{34} = \begin{cases} 1 - k_{23}, & \text{if } n = 0, \\ -k_{34}(1 - k_{23}), & \text{if } n = P_4, \\ 0, & \text{if } n \neq 0 \neq P_4, \end{cases}$$

where P_1 and P_4 are positive integers and

$$k_{ij} = \frac{\rho_i - \rho_j}{\rho_i + \rho_j}, \quad i, j = 1, 2, 3, 4.$$

The curve-fitting method is also applicable for multi-layered models. For parameters of the curves one can select the thickness of the seam and of the beds, and the ratio of resistivities. According to (2) the apparent resistance of the multi-layered series can also be determined.

The apparent resistivity measured by the seam-sounding method within the drift is

$$\rho_a = 2\pi \frac{r(r^2 + b^2)^{1/2}}{(r^2 + b^2)^{1/2} - r} \cdot R_s, \tag{3}$$

where R_s is calculated from (2). A typical set of curves is seen in fig. 4.

The resolution of the geoelectric seam-sounding and transillumination methods can be better analyzed if one considers the resistivity curves together with the

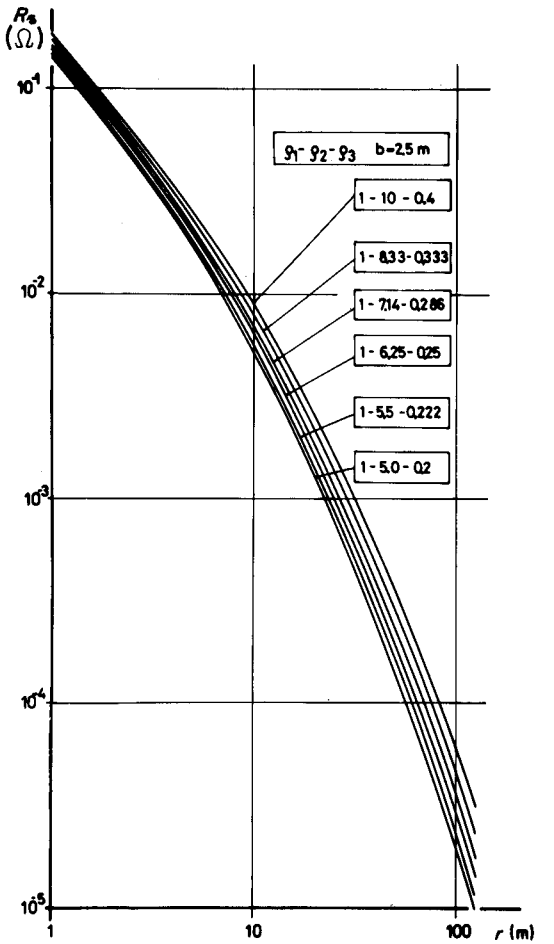

Fig. 3. Resistance master curves for seam-soundings, three layers.

apparent resistance curves. For example, it follows from (1) and (3) that

$$\lim_{r\to\infty} \rho_a = \frac{2\rho_2^2}{\rho_1 + \rho_3}, \tag{4}$$

that is, in case of large dipole arrays the apparent resistivity measured by seam-sounding is mainly determined by the true resistivity of the coal bed. At large distances the relative change in apparent resistivity ρ_a is much greater than the relative changes in the resistivity of the coal bed ρ_2. This can be seen in the following example.

For $\rho_1 = \rho_3 = 10\ \Omega$m and $\rho_2 = 200\ \Omega$m, one has $\lim_{r\to\infty} \rho_a = 4000\ \Omega$m; for $\rho_1 = \rho_3 = 10\ \Omega$m and $\rho_2 = 150\ \Omega$m, we have $\lim_{r\to\infty} \rho_a = 2250\ \Omega$m.

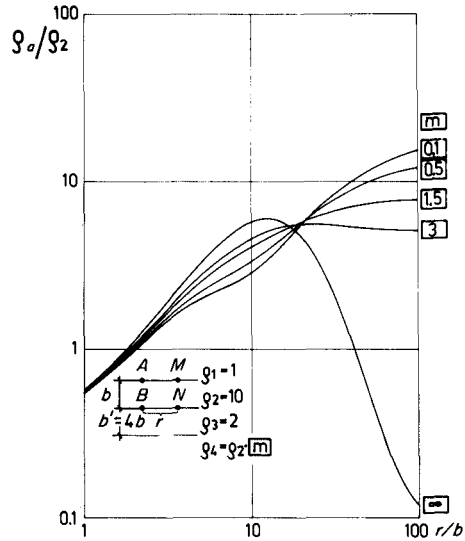

Fig. 4. Resistivity master curves for seam-soundings, four layers.

Determination of the Parameters of the Undisturbed Model

In order to interpret the data of in-seam geoelectric measurements we must know the apparent resistivity of the undisturbed model. This can be determined by statistical methods from data of seam-sounding measurements, or it can be computed using (1), (2), (3) if one knows the values of the resistivities and thickness figuring in those formulae. The parameters of the host rock can also be determined by drift-sounding (Gyulai 1982). In these measurements vertical geoelectric soundings are carried out using gradient array either at the floor of the drift (floor-sounding) or at the roof (roof-sounding). The measured apparent resistivity can be plotted against distance $r = AB/2$ in the usual way on a log–log scale. Because of its high resistivity, the coal seam has a current-deflecting effect. The apparent resistivity can be calculated from the measured data (U, I) as

$$\rho_a = 2\pi \frac{r^2}{b} \cdot \frac{U}{I}. \tag{5}$$

One has the following formula for roof-sounding in a three-layer model:

$$\rho_a(\text{roof}) = \rho_1 \left\{ 1 + k_{21} \sum_{n=0}^{\infty} \frac{(k_{21}k_{23})^n r^3}{[4n^2b^2 + r^2]^{3/2}} - k_{23} \sum_{n=0}^{\infty} \frac{(k_{21}k_{23})^n r^3}{[4(n+1)^2b^2 + r^2]^{3/2}} \right\}, \tag{6}$$

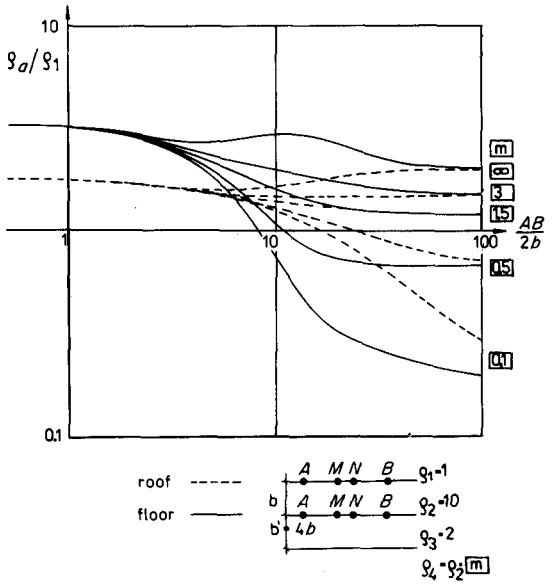

Fig. 5. Master curves for drift-soundings, four layers.

while the floor-sounding curve is described in the three-layer model:

$$\rho_a(\text{floor}) = \rho_3\left\{1 + k_{23}\sum_{n=0}^{\infty}\frac{(k_{21}k_{23})^n r^3}{[4n^2b^2 + r^2]^{3/2}} - k_{21}\sum_{n=0}^{\infty}\frac{(k_{21}k_{23})^n r^3}{[4(n+1)^2b^2 + r^2]^{3/2}}\right\}. \tag{7}$$

Formulae can also be derived for the multilayer case. The parameters of the layers can be obtained either by fitting curves calculated from model-formulae (fig. 5) or by direct evaluation programs (Koefoed 1979, Gyulai 1982).

The apparent resistivity of the undisturbed coal series can be calculated for any dipole distance r using the above formulae. From (4) and (5) it easily follows that in the full space

$$\lim_{r\to\infty}\rho_a = 2\frac{\rho_1\rho_3}{\rho_1 + \rho_3}, \tag{8}$$

i.e., at great dipole distances the apparent resistivity of the coal series obtained from drift-sounding would be equal to the mean value of the resistivities of the embedding strata. Contrary to seam-sounding, in case of drift-sounding with great dipole distances, the coal seam appears to be an infinitely thin and large plate. Consequently, the tectonic and stratigraphic disturbances of coal-seams are not detectable by the usual VES measurements. However, seam-sounding and transillumination methods are sufficiently sensitive in order to detect disturbances within the seam.

Maps of Deviations Between Measured and Computed Values

For a convenient and easy interpretation of the seam disturbances the deviations found between measured and computed apparent resistances should be superimposed—in a contour map form—over the mining map. The measured values of the apparent resistance should be drawn perpendicularly to the midpoint of the dipole array r in the plane of the seam, at a distance r from the drift, as seen in fig. 6.

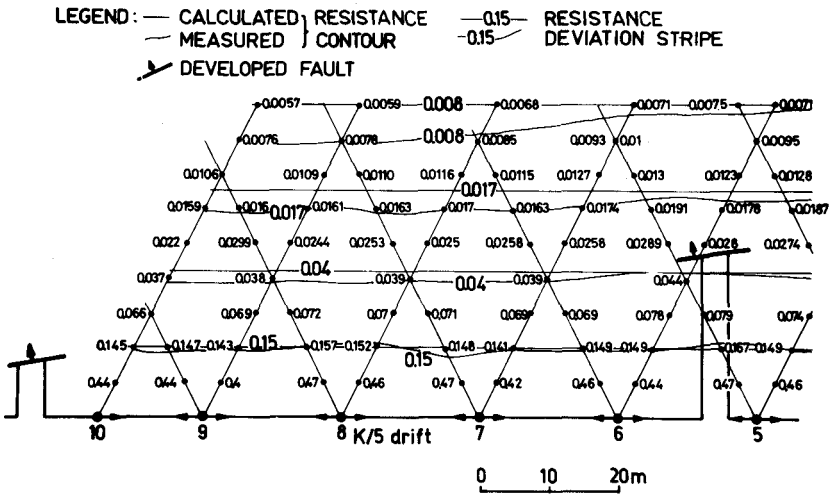

Fig. 6. Resistance map.

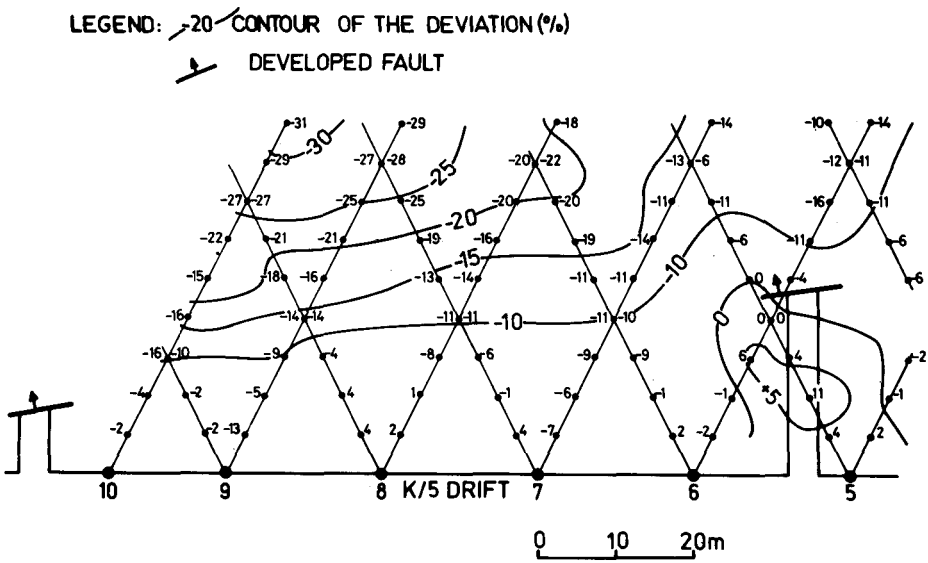

Fig. 7. Resistivity deviation map determined from seam-sounding.

The contours of the undisturbed resistance model are parallel to the drift. The distance between them does not change if their values logarithmically decrease as a function of the distance from the drift. The measured and computed contours, respectively, of the same values do not agree any more at zones of seam disturbances. The stripes between them are wider where the slip is greater and where the fault zones are broader.

The disturbed zones are easily visualized by the contours of relative deviations $E\%$ between the measured and computed apparent resistivities as seen in fig. 7. Around the drift tunnel a resistivity increase of $+4$ to $+11\%$ can be observed. This is caused by the fact that the drift serves as a space of infinite resistivity.

Transillumination and Geoelectric Imaging

Openings are usually driven into coal beds as counter-gangway. In this case the tectonic disturbances of coal seams can also be investigated by means of seam-transillumination. In seam-transillumination the current dipoles are placed in one of the drifts and the potential dipoles in the other one so that the rays connecting the dipoles should cover the coal bed in a fan-shaped form. The apparent resistance of a layered model can be computed if the resistivities and thickness of the layers as well as the dipole distance are given. The apparent resistance of the undisturbed strata can also be determined by a statistical method from the seam-transillumination data.

Seam disturbances are found along those rays where the measured resistance data are smaller than the computed ones. Because of the large resistivity contrast between coal bed and adjacent rocks, the apparent resistance is determined by the true resistivity distribution of the coal bed. The resistivity of the coal bed is around $\rho_2 = 200\ \Omega\text{m}$ and of the adjacent strata: $\rho_1 \approx \rho_3 \approx 10\ \Omega\text{m}$.

The seam-transillumination data can be processed with a geoelectric resistivity imaging method (see the appendix). Figure 8 shows the distribution of the relative deviations of the local apparent resistivity of a coal field. The faults detected by drifts are indicated by contour values that increase with the net slip and the amount of tectonization. The fault zones discovered during the excavation are shown by

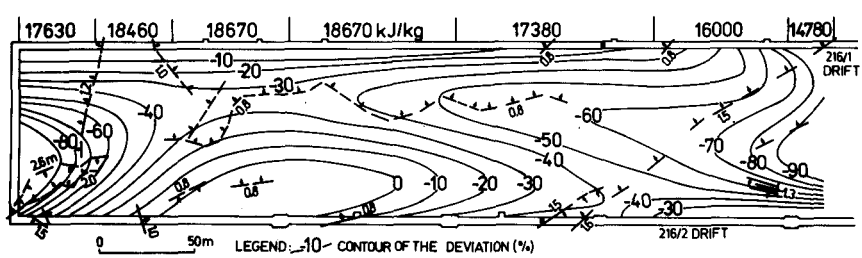

Fig. 8. Resistivity deviation map determined from seam-transillumination.

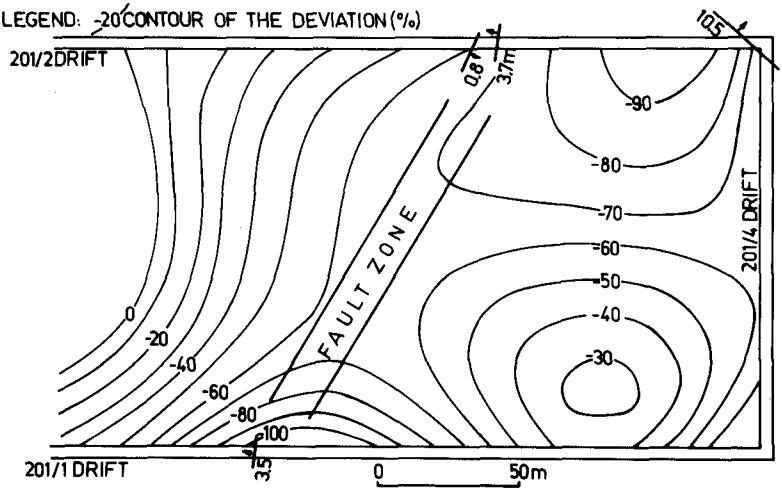

Fig. 9. Resistivity deviation map and prediction of faults determined from seam-transillumination.

contours similarly to the tectonic style. Figure 9 shows the geoelectric image of an other coal field. On the geophysical mining map contour lines correspond to the localization of the faults. The apparent resistivity decrease is as high as −90% in fault zones.

Geoelectric Transillumination and Seismic Absorption Tomography

As is shown in fig. 8 and fig. 9 the proposed geoelectric resistivity imaging method results in maps comparable with the ones found in seismic tomography.

It is known from seismic wave-propagation theory literature that the absorption of the seismic waves is the most sensitive indicator of the petrologic changes. By means of the seismic tomographic method we can map the distribution of the absorption coefficients obtained from seismic transmission measurements (Dobróka 1985). In the absorption maps fault zones are indicated by high values of the absorption while the ribbed coal seam are indicated by low values. The seismic transmission measurements were carried out in the coal field for which the geoelectric resistivity map was shown as fig. 9. The tomographic map of the distribution of the absorption coefficients [$1/m$] in the detected coal bed can be seen in fig. 10. The fair correlation between geoelectric resistivity contours and the contours of the seismic absorption coefficient is seen by comparing fig. 9 and fig. 10. The tectonic style of the strata appears in a fully comparable form both on the geoelectric and the seismic maps. Examination of the contours proves that the zone of the fault with a slip of $H = 3.5$ m, developed by drift tunnel, passes through the coal seam by the side of the contours of a resistivity decrease of 70–100% and of the absorption-factor contour marked 60. It can also be seen that a fault with a slip of

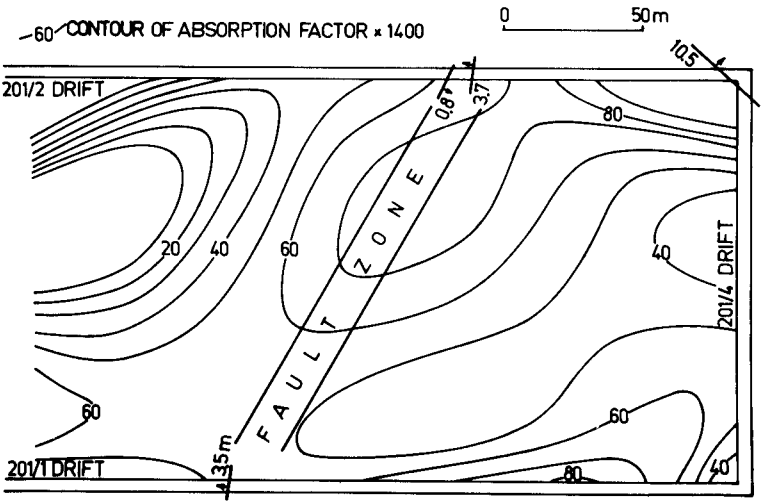

Fig. 10. Map of the seismic absorption factor obtained by in-seam tomography. Contour values are 1400 × absorption factor.

$H = 10.5$ m causes a resistivity decrease of -90% (figs 9 and 10), and an absorption high (90). According to the complex evaluation of the geoelectric and the seismic methods, the following interpretation rule has been formed:

1. where both the resistivity decrease and the absorption factor have large values, the tectonization is strong;
2. where there is a larger resistivity decrease but only a small absorption factor, a ribbed coal seam or a growing barreness should be expected.

Determination of the Caloric Value

The caloric value of brown coal beds can be related to their resistivity, because the resistivity of the coal seams decreases with growing ash content and the middleman (Kayal and Das 1981). This relationship is close if the qualities of the ash content, of the middleman and the moisture content are constant in the coal seam. Figure 8 shows the contour map of the apparent resistivity distribution within a coal seam obtained by geoelectric imaging. Geologists of the Mining Company provided us with caloric values of the excavated parts of the coal field indicated on the top line of fig. 8. Since the caloric values shows a correlation with the electric resistivity in an undisturbed coal bed, it is reasonable to expect that its distribution should be related to the relative deviation $e(x, y)$ (see appendix) of the apparent resistivity in a disturbed coal bed as well. Figure 11 shows the behaviour of the $A[\text{kJ kg}^{-1}]$ average per tract and the $\tilde{e}$ average per tract along the drift. The interrelation of the seven related pairs $\tilde{e} - A$ is seen on the right-hand side of fig. 11. The functional form of the relation between quantities $\tilde{e}\%$ and A can be expressed as

$$A[\text{kJ kg}^{-1}] = 19\,100 - 0{\cdot}68(\tilde{e}\%)^2. \tag{9}$$

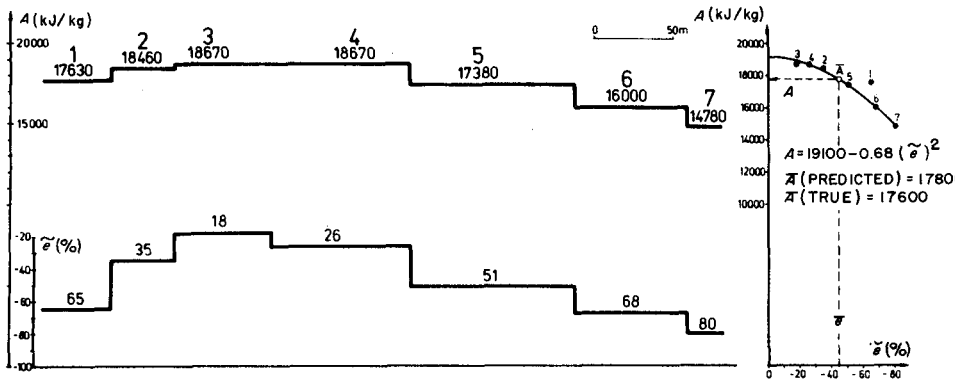

Fig. 11. Relation between the resistivity deviation and the caloric value of the coal bed.

It is also seen, that the pairs $\bar{A}$ (mean caloric value of the total face) and $\bar{e}$ (mean relative deviation of the apparent resistivity computed for the total investigated area) are close to the computed curve. This yields a possibility for estimating the mean caloric value by means of geoelectric measurements before the excavation.

Point #1 does not lie on the curve because a fault zone penetrates tract #1 with a slip of $H = 2.0$–2.6 m (fig. 8). In this tract the relative deviation of the apparent resistivity is highly influenced by the faults.

Conclusions

Methods of geoelectric seam-sounding and transillumination can detect coal seam disturbances, and a novel method of geoelectric imaging has been shown.

These methods were illustrated by in situ measurements in coal seams. The results show that these methods can not only be used to detect faults of the coal series, but also to investigate quality changes of the coal seam and to predict the mean caloric value of the coal. A joint application of the proposed methods together with seismic in-seam tomography gives further information for the interpretation of the measurements.

Acknowledgments

Special thanks are due to Mr A. Varga and to Mr Gy Gondozó from Oroszlány Coal Mine (Hungary) for their kind help in all stages of this project.

Appendix

A geoelectric imaging method

The electric imaging methods enable one to determine the variations of the electrical conductivity by means of resistance measurements (Dines and Lytle 1981). Using the geoelectric transmission method the apparent resistance can be measured. Its varia-

tions are determined by the inhomogeneities of the medium. In order to determine the distribution of these inhomogeneities we have developed a simple way of geoelectric imaging. Usually the resistivity of the coal deposit is much higher than that of the adjacent layers. Consequently, the variations of apparent resistivity are mainly influenced by the inhomogeneities of the coal deposit. In order to describe the distribution of the inhomogeneities we introduce the local apparent resistivity $\rho_a(x, y)$ as

$$R_a^{(k)} = \frac{U_{AB}^{(k)}}{I_k} = \frac{1}{K(r)A_k} \int_{L_k} \rho_a \, dA_k, \tag{A1}$$

where L_k is the surface of integration lying in the plane of the coal seam, A_k is its area, $K(r)$ is the geometrical factor. The surface A_k is extended to that range of the plane of the seam, where the inhomogeneities appreciably contribute to the change of the apparent resistance. In the relative deviations of the apparent resistance we can write

$$E_k = \frac{1}{A_k} \int_{L_k} e(x, y) \, dA_k, \tag{A2}$$

where $e = (\rho_a - \rho_a^{(0)})/\rho_a^{(0)}$, $\rho_a^{(0)}$ is the apparent resistivity computed for the undisturbed medium. The distribution of the inhomogeneities can be written in the form

$$e(x, y) = \sum_{n=1}^{N} \sum_{m=0}^{n} B_j T_{n-m-1}(x) \cdot T_m(y), \tag{A3}$$

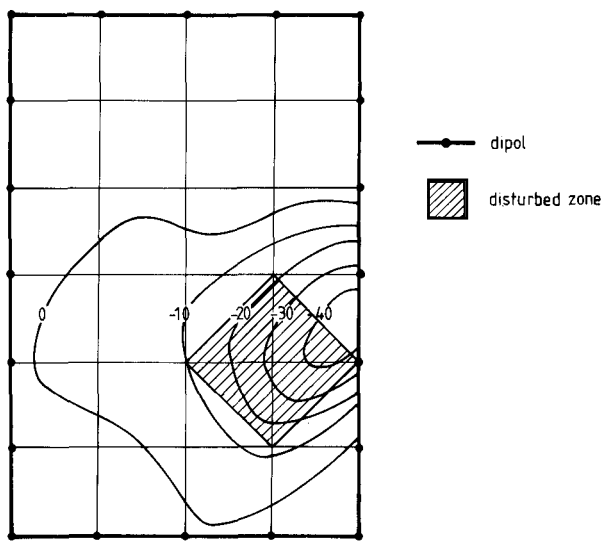

Fig. 12. The model and the reconstructed $e(x, y) \cdot 100$ distribution.

so that by (A2) we have

$$E_k = \sum_j B_j S_{kj}, \tag{A4}$$

where $j = [n(n-1)/2] + m + l$, T_m are mth order Chebyshev-polynomials and

$$S_{kj} = \frac{1}{A_k} \int_{L_k} T_{n-m-1}(x) T_m(y)\, dx\, dy. \tag{A5}$$

Equation (A4) yields an overdetermined set of equations for the coefficients B_j that can be solved by the least mean squares method. In terms of the computed values of B_j the distribution of the inhomogeneities can be expressed by means of (A3).

The geoelectric imaging algorithm presented here has also been tested in a model measurement. In this experiment the coal bed was substituted by a cement sheet of 140 Ωm resistivity. The current and measuring electrodes, as well as (in order to represent the low resistivity inhomogeneity of the bed) two copper sheets short-circuited electrically to each other were glued to the surfaces of the cement sheet as shown in fig. 12. The measurement was carried out in a tank filled with an electrolyte of 10 Ωm resistivity. From the apparent resistivity data measured on the homogeneous model (without the copper sheet) and on the inhomogeneous one we formed the quantities

$$E_k = \frac{R_k\,(\text{inhomog}) - R_k\,(\text{homog})}{R_k\,(\text{homog})}. \tag{A6}$$

Starting out from these input data we reconstructed the $e(x, y)$ distribution of the apparent resistivity inhomogeneities, using the presented geoelectric imaging method. The results shown in fig. 12 prove that the geoelectric imaging method can successfully reconstruct the place of the inhomogeneities.

REFERENCES

CSÓKÁS, J. 1974, Detection of tectonic disturbances associated with a coal bed by geoelectrical measurements in mine drifts, Acta Geodaetica Geophysica et Montanistica Hungarica, 111–119.

DINES, K.A. and LYTLE, R.J. 1981, Analysis of electrical conductivity imaging, Geophysics 46, 1025–1036.

DOBRÓKA, M. 1985, Love seam-waves in a horizontally inhomogeneous three-layered medium—an amplitude inversion method, paper at the 47th EAEG meeting, Budapest, June 1985, Geophysical Prospecting (in revision).

DRESEN, L. and FREYSTÄTTER, ST. 1976, Rayleigh channel waves for the in-seam seismic detection of discontinuities, Journal of Geophysics 42, 111–129.

GYULAI, A. 1982, Interpretation of in-mine geoelectric soundings by means of kernel functions, Eötvös Loránd Geophysical Institute of Hungary, Geophysical Transactions 28, 47–56.

KAYAL, J.R. and DAS, L.K. 1981, A method of estimating ash content of coal from combined resistivity and gamma-ray logs, Geoexploration 17, 193–200.

KOEFOED, O. 1979, Geosounding Principles, 1. Resistivity Sounding Measurements. Elsevier, Amsterdam.

KREY, TH., ARNETZL, H. and KNECHT, M. 1982, Theoretical and practical aspects of absorption in the application of in-seam seismic coal exploration, Geophysics 47, 1645–1656.

MASON, I.M., BUCHANAN, D.J., BOVER, A.K. 1980, Channel wave mapping of coal seams in the United Kingdom, Geophysics 45, 1131–1143.

VAN NOSTRAND, R.G. and COOK, K.L. 1966 Interpretation of Resistivity Data, US Government Printing Office, Washington, 134–135.